Mechanism of the Wacker Oxidation of Alkenes over Cu-Pd-Exchanged Y Zeolites

P. H. Espeel, G. De Peuter, M. C. Tielen, and P. A. Jacobs*

Centrum voor Oppervlaktechemie en Katalyse, K. U. Leuven, 92, Kardinaal Mercierlaan, B-3001 Heverlee (Leuven), Belgium

Received: June 11, 1994; In Final Form: August 26, 1994[⊗]

The catalytic potential of CuPd zeolites with faujasite topology in the Wacker oxidation of 1-alkenes with dioxygen is reported and compared with that of a homogeneous $PdCl_2$-$CuCl_2$ salt solution. The influence of water, oxygen, and alkene partial pressure on the rate of oxidation and the use of different alkenes and perdeuterated ethene as substrate allowed to establish similarities between the heterogeneous and homogenous system as well as specific zeolite effects. *In situ* IR and ESR spectroscopy of a working catalyst allowed to propose an active site consisting of a trinuclear Cu-O-Pd-O-Cu cationic complex and a catalytic cycle for the Wacker oxidation in which the reoxidation of Cu^+ by dioxygen or of Pd^0 by zeolite Cu^{2+} is rate determining. Diagnostic probing of the phenomena with CO in IR and ESR confirmed this picture.

Introduction

Most large scale synthesis of aldehydes and ketones occurs either via a two-step process in which alkenes are hydrated to alcohols and subsequently dehydrogenated to the corresponding carbonyl compounds[1,2] or via a one-step process developed by Smidt et al.[3] and presently known as the Wacker or Wacker-Hoechst oxidation. The latter process performs the direct oxidation of ethene and other olefins with dioxygen in the presence of aqueous acidic solutions of $PdCl_2$ and $CuCl_2$ at pH $\leq$ 1.4.

The overall chemistry of a Wacker oxidation consists first in the activation of the alkene through coordination with a Pd^{2+} cation, thus allowing nucleophilic attack of water on the alkene and reducing Pd^{2+} to Pd^0. In a second step Pd^0 is reoxidized with the help of the Cu(II)/Cu(I) redox couple. Finally, cuprous ions are reoxidized with dioxygen. Thus, an inorganic electron transfer chain transfers electrons from the alkene substrate to dioxygen using Pd(II)/Pd(0) and Cu(II)/Cu(I) redox couples. This sequence of steps is known as the Wacker concept[4] and is schematically represented in Figure 1.

Homogeneous Wacker chemistry suffers from serious technical and environmental drawbacks including the separation of the catalyst from the product, the formation of chlorinated byproducts, and the corrosive environment associated with the low pH of the catalyst solution and the chloride medium. As a result, attempts have been published to heterogenize Wacker catalysts. They include the use of supported liquid-phase catalysts,[5] of supported molten salt catalysts,[6] and of micas and zeolites,[7-11] all containing the Cu/Pd ion pair. An alternative approach has been the use of bulk or supported V_2O_5 impregnated with a palladium salt.[12-15] Homogeneous chloride-free systems typically comprise a palladium salt and a salt of a heteropoly acid.[16,17]

Several authors have reported the use of Pd(II)/Cu(II) exchanged in Y-zeolites for the heterogeneous Wacker oxidation of ethene and propene.[7-10] Based on product similarity and the synergy between zeolitic Pd and Cu, Arai et al. tentatively advanced a reaction mechanism identical to that established for the homogeneous phase.[9] As in most studies, Pd^{2+} ions were exchanged in the zeolite using the tetraammine complex, it was certified that no residual ammonia was present in a working catalyst.[7-10] Alternatively, Minachev et al. were comparing Wacker chemistry with $PdCl_2$- and $CuCl_2$-impregnated supports and reported the superior behavior of zeolites.[18-21]

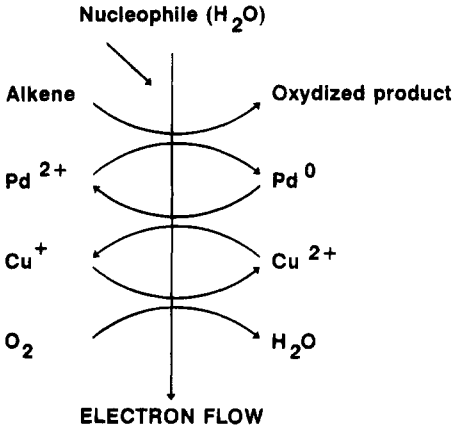

Figure 1. Schematic representation of the Wacker concept.

Despite these experimental efforts, no attempt has been made to understand in detail Wacker chemistry with Cu/Pd zeolites. In a preliminary communication[22] we reported that Cu/Pd zeolites are superior catalysts in the ethene oxidation provided that (i) faujasite is the zeolite topology used for cation retention, (ii) two residual NH_3 ligands are present to stabilize Pd, and (iii) the atomic Cu/Pd ratio is 2. Based on isotope incorporation experiments, it was also shown that the acetaldehyde oxygen atom stems from water rather than from dioxygen and that only internal hydrogen was involved in the rearrangement of coordinated ethene into acetaldehyde.[22] All these similarities supported the conclusion that the oxidation mechanism should be similar in chloride and zeolitic environment.

As prior work does not allow to locate with certainty the rate-determining step in the catalytic cycle, to describe the nature and regeneration of the active site, and to make generalizations as far as the nature of the alkene is concerned, it is the purpose of the present study to characterize the active site and investigate the electron-transfer chain in detail for several alkenes, in order to establish accurately similarities and differences between homogeneous and zeolite-based Pd/Cu Wacker catalysts.

Results

Requirements for High Catalyst Activity and Stability in the Oxidation of Ethene to Acetaldehyde. Figure 2 represents

[⊗] Abstract published in *Advance ACS Abstracts,* October 1, 1994.

0022-3654/94/2098-11588$04.50/0

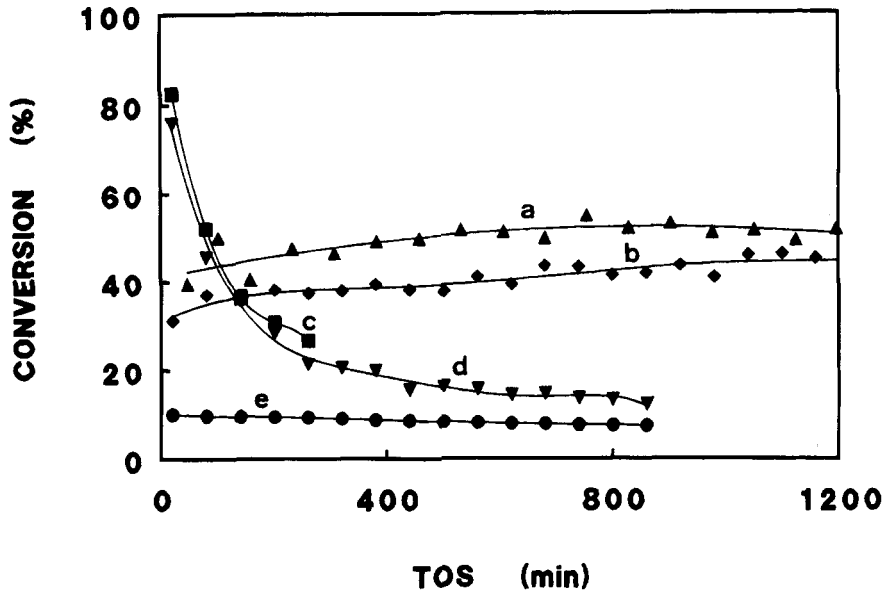

Figure 2. Ethene conversion vs. time on stream (TOS) over zeolite 12Cu06PdY. The catalyst was precalcined under a flow of 60 mL/min of oxygen at (a) 373 K, (b) 473 K, (c) 573 and (d) 673 K. The reaction temperature was 373 K, the total space–time (W/F_0) 2.86 kg·s·mol^{-1}, with a water partial pressure of 14 kPa and an ethene/dioxygen molar ratio of 19. For curve *e* the dioxygen partial pressure was changed as to have a substrate/oxydans molar ratio of only 1.

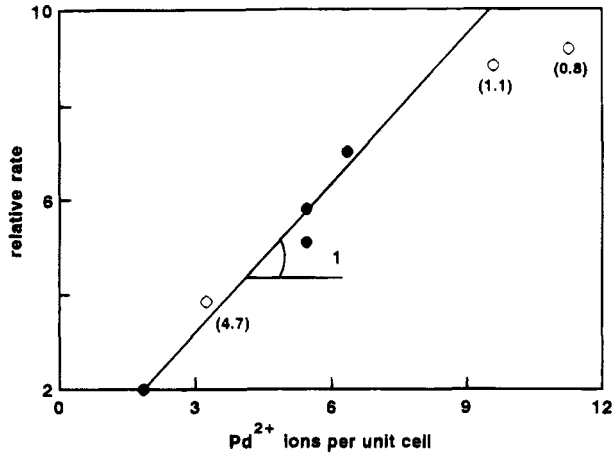

Figure 3. Dependence of the steady-state reaction rate in standard conditions on the amount of Pd in the catalyst at Cu/Pd ratios of 2 or lower (open symbols with values in brackets).

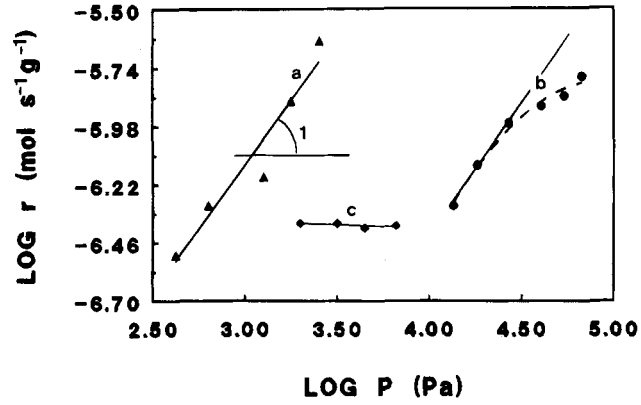

Figure 4. Dependence of the steady-state oxidation rate of ethene (a, b) and propene (c) over 12Cu06PdY on the partial pressure of oxygen (b), ethene (a), and propene (c) in otherwise *standard* reaction conditions.

for ethene oxidation with the *standard catalyst* (12Cu06PdY) the influence of the oxygen precalcination temperature and the oxydans to substrate molar ratio on the activity and stability in time. With high oxydans to substrate molar ratios, pretreatments below 473 K hardly change catalyst activity and stability. Precalcination above 573 K dramatically reduces catalyst stability. The high initial activity of the latter catalysts is only the result of an increased yield in carbon oxides. With low oxydans to substrate molar ratios, low catalyst activity is observed. Finally, pretreatments under nitrogen (between 573 and 673 K) or ethene (at 373 K) produce an inactive zeolite as well.

Mass spectrometric monitoring (at $m/e = 17$) of the reactor exit during precalcination indicates that ammonia release from the sample starts only from 423 K onwards, indicating that the active catalysts retain all ammonia. Oxidative decomposition of ammonia (at $m/e = 30$) only starts at 573 K.

In Figure 3 relative rates of ethene oxidation at steady conversion are represented for increasing loadings of Pd either at constant or variable Cu/Pd ratios in zeolite Y. For the catalysts with a Cu/Pd ratio equal to 2, the reaction rate is directly proportional to the number of Pd ions per unit cell, indicating that the turnover number frequency of a $Cu_{2n}Pd_nY$ zeolite (i.e., the rate per Pd ion) is constant irrespective of its Pd loading. For variable Cu/Pd ratios, this is only true when this ratio is 2 or higher. When the Cu/Pd ratio of the catalysts is progressively decreased, the turnover number frequency decreases. Clearly, the active site for ethene oxidation with dioxygen requests the presence of at least two Cu ions per Pd ion.

Kinetics of Alkene Oxidation. Ethene, propene, and 1-butene were oxidized with dioxygen separately or as binary mixture. In every case the selectivity for the Wacker product (acetaldehyde, acetone, or butanone, respectively) was always over 90%.

Figure 4 shows a logarithmic plot of the ethene oxidation reaction rate on the standard catalyst against the partial pressures of C_2H_4 and O_2. The observed first order in ethene (Figure 4a) is in agreement with the kinetics obtained in chloride medium.[23] The order in propene in similar conditions is close to zero (Figure 4c). The order in oxygen only tends to zero at the higher oxygen partial pressures. At lower partial pressures of oxygen, the reaction order is close to one (Figure 4b). This implies that

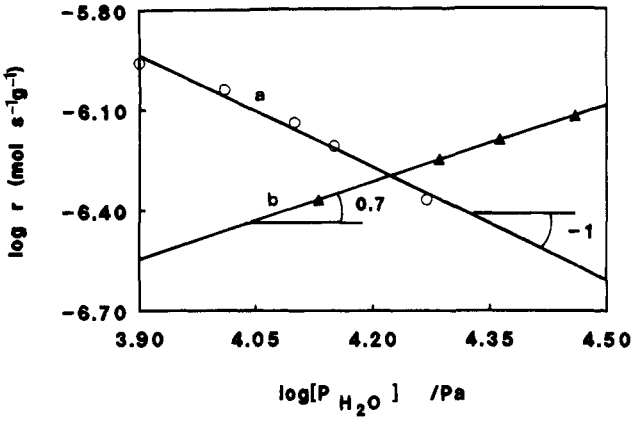

Figure 5. Ethene (a) and propene (b) oxidation rate against the partial pressure of water, for otherwise *standard* reaction conditions.

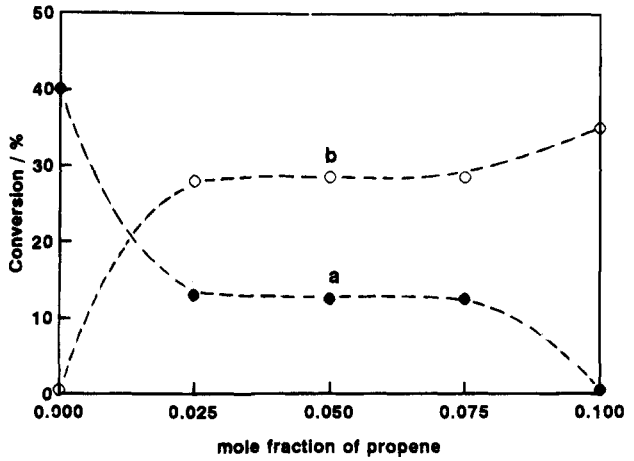

Figure 6. Steady-state oxidation conversion of ethene (a)−propene (b) mixtures with increasing amounts of propene on 14Cu03PdY; the reaction temperature is 373 K, the space time 2.86 kg·s·mol^{-1}; the volumetric feed consists of 40.1% of dioxygen, 19.1% of water, 2.1% of alkenes, and 38.6% of helium.

the rate-limiting step is gradually changing with the oxygen partial pressure. In homogeneous Wacker chemistry this order is always zero.[23]

In homogeneous Wacker oxidations, water is available in excess and no influence on the reaction rate is expected. Although there is no net consumption of water (Figure 1), in the present case a 4-fold volumetric excess of water with respect to ethene is necessary to guarantee catalyst stability in time. A further increased partial pressure of water (between 10 and 32 kPa) shows an order of almost −1 (Figure5a). As the activity reversibly changes when the water partial pressure is decreased again, the existence of strong competitive adsorption of water for ethene is obvious.[24] In the same range of water partial pressures, the order in water is 0.7 for propene oxidation (Figure 5b), indicating that propene is adsorbing more strongly than ethene. It cannot be excluded that competitive adsorption between water and alkenes occurs in the zeolite cages rather than in the coordination sphere of Pd.

The existence of competitive sorption is confirmed when alkene mixtures are fed to the catalyst. Figure 6 gives the ethene and propene oxidation rate when increasing amounts of propene are mixed with the ethene substrate. In comparable conditions pure ethene is oxidized more rapidly than propene. However, when more propene is present in the alkenes mixture, a Langmuir-type dependence is found for the rates, the more strongly adsorbing propene suppressing significantly the oxidation of ethene. This behavior is general as for mixtures of

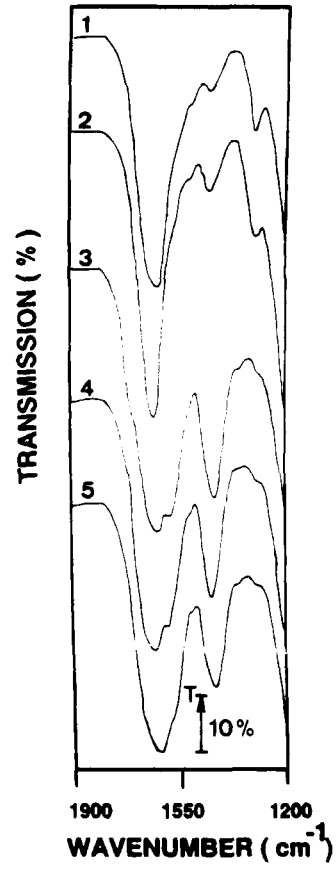

Figure 7. *In situ* IR behavior of 12Cu06PdY at a water vapor pressure of 2.4 kPa. IR spectrum before reaction (1) and after 5 (2), 60 (3), 120 (4), and 360 (5) min of reaction in otherwise *standard* conditions.

propene and 1-butene; the presence of the latter olefin also significantly suppresses propene oxidation. Therefore, the alkene concentration available for coordination with Pd^{2+} is directly determined by the concentration in the zeolite pores and only indirectly by their partial pressure.[25]

The ratio of the oxidation rates of ethene and ethene-d_4 in *standard conditions* with the *standard catalyst* was 1.1, which is close to value obtained in the homogeneous case,[3b,c] and points to the absence of a major isotope effect.

Spectroscopic Characterization of the Electron-Transfer Chain. As the IR behavior of $Pd(NH_3)_4^{2+}$ in CuY zeolite has not been investigated before, an *in situ* IR characterization of a working catalyst was performed at low partial pressure of water vapour (2.4 kPa), so as to induce gradual catalyst deactivation. The IR spectrum of as-synthesized 12Cu06PdY (Figure 7, spectrum 1) shows distinct bands at 1310, 1455, and 1635 cm^{-1}, assigned to the symmetric deformation of NH_3 coordinated to Pd^{2+}, the N−H deformation of NH_4^+ ions, and the deformation vibration of physisorbed water, respectively. No N−H deformation band of $Cu(NH_3)_4^{2+}$ is present, which is reported at 1275 cm^{-1} in CuY[26] and consequently no ammonia is transferred from Pd^{2+} to Cu^{2+} in reaction conditions. The *in situ* IR behavior of the deactivating catalyst (Figure 7, spectra 2−5) shows a continuous decrease in intensity of the 1310 cm^{-1} band and a parallel increase in intensity of the NH_4^+ band. A shoulder at 1577 cm^{-1} assigned to $\nu_{C=C}$ of coordinated ethene is more pronounced on a more deactivated catalyst. When the same experiment is performed in catalytically stable conditions (e.g., with partial pressure of water of 7 kPa) the intensity of all bands hardly changes. This indicates that during catalyst deactivation Pd ions are progressively reduced by ethene, and released ammonia ligands are taken by protons from water dissociation.

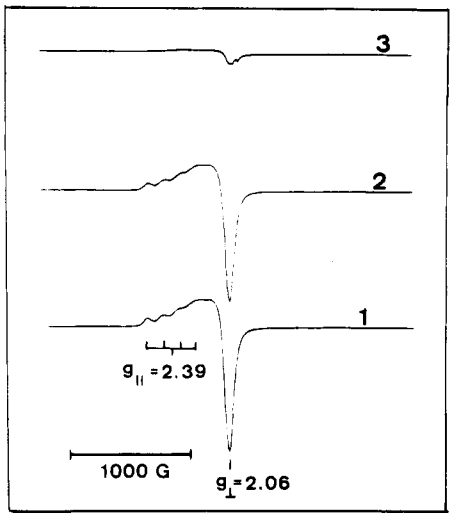

Figure 8. ESR spectra obtained at 120 K of fresh 12Cu06PdY (1), after exposure of (1) to 10 kPa ethene for 60 min (2), and of (2) to the *standard* reaction atmosphere always at room temperature (3).

Consequently, Cu^{2+} ions in absence of sufficient water are unable to reoxidize reduced Pd. The role of water possibly is to enhance the mobility of the Cu^{2+} ions and to keep them in the immediate neighborhood of Pd.[27]

Addition in reaction conditions of excess ammonia to a precalcined catalyst shows the symmetric deformation of NH_3 coordinated to Cu^{2+} (1275 cm^{-1}), a very large NH_4^+ band (1455 cm^{-1}) and the complete absence of the symmetric N−H deformation of Pd-ammine (1310 cm^{-1}). Apparently, Cu^{2+} ions are abundantly present in a deactivated catalyst[28] but are unable to reoxidize reduced Pd.

ESR spectroscopy with 12Cu06PdY can be used to follow the electron transfer from reduced Pd to Cu^{2+} and oxygen, as it allows to monitor the disappearance of the Cu^{2+} signal and the eventual formation of Pd^+. Figure 8 shows the ESR spectra of a hydrated 12Cu06PdY before and after room temperature admission of ethene. Initially, only a single signal with $g_{\|} = 2.39$, $g_{\perp} = 2.06$ and $A_{\|} = 0.129$ T is observed, which is assigned to hydrated Cu2+ ions.29b−d Upon room temperature admission of 10 kPa of ethene, Cu^{2+} still remains the only paramagnetic species30 and is present with unreduced intensity. After 1 hour of exposure, only 10% of Cu^{2+} is reduced. During this process the sample progressively changes color from light green to gray and $Pd(NH_3)_42+$ is progressively reduced as was shown by IR spectroscopy (Figure 7). All this shows that upon room temperature treatment of 12Cu06PdY with ethene, Pd^{2+} is reduced to Pd^0 but Cu^{2+} is left almost untouched. It implies that Cu^{2+} is unable to reoxidize Pd^0 at room temperature as was already derived from the IR data. When this catalyst is contacted at room temperature with the reactants for ethene oxidation (Figure 8, spectrum 3), a strong reduction of the Cu^{2+} signal is observed, which is only complete after 1 h, indicating that in the reaction atmosphere at room temperature Cu^{2+} ions only are able to slowly reoxidize Pd^0.

Spectroscopic Characterization of the Electron Transfer Chain in Presence of CO as Diagnostic Probe. Carbon monoxide can be used to probe the simultaneous presence of different redox states of Pd and Cu and consequently to characterize the electron-transfer chain. Indeed, a possible transfer of electrons from Pd^0 to Cu^{2+} or Pd^{2+}, leading to the formation of Cu^+ and/or Pd^+ should be visible. In order to reach a better understanding of the IR spectra of CO adsorbed on hydrated CuPdY zeolites, the spectra of hydrated PdY and CuY were studied upon admission of 3 kPa of CO. On hydrated

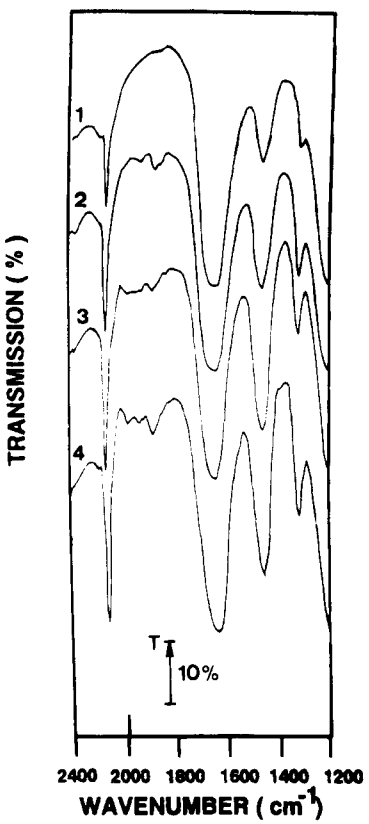

Figure 9. IR spectra of (1) 03Cu02PdY, (2) 06Cu03PdY, (3) 09Cu04PdY, and (4) 12Cu06PdY immediately after admission of 3 kPa of CO at room temperature.

PdY only very weak IR bands appear which are similar to those found for a reduced dehydrated PdY,[31] but of much lower intensity. Their assignment is irrelevant for the present discussion. A CuY did not show any measurable CO adsorption capability at 293 K. Only after a considerable equilibration time a band at 2135 cm^{-1} appeared, which in agreement with earlier work[32] is attributed to Cu^+−CO species.

Figure 9 shows that the introduction at 298 K of 3 kPa of carbon monoxide on hydrated CuPdYsamples immediately results in the formation of a strong band at 2121 cm^{-1}, the intensity of which increases with the Pd content of the sample. Variations in the intensity of this vibration and the ammonium band occur in parallel. At the same time, weak bands around 1970, 1900, and 1830 cm^{-1} appear. On PdNaY, similar bands below 2100 cm^{-1} but of much higher intensity have been observed after reduction.[31] These changes are amplified for longer equilibration times (spectra not shown), indicating that CO is not a neutral probe but reduces Pd^{2+} ions. Mass spectrometric analysis of the fate of CO shows that after equilibration CO_2 is formed with all samples in quantities proportional to the Pd^{2+} content of the zeolite (when the amount of Pd is doubled, also the *m/e* abundance at 44, is doubled). This implies that at room temperature CO reduces Pd^{2+} in the presence of water upon formation of CO_2. As the intensity of the ammonium band and the amount of CO_2 formed after CO exposure is proportional to the Pd^{2+} content of the zeolites, it seems that CO reduced Pd is not regenerated by zeolitic Cu^{2+} at room temperature and consequently that regeneration of reduced Pd by Cu^{2+} will also be slow in reaction conditions.

Figure 10 shows that CO admission at room temperature to hydrated 12Cu06PdY does not change the ESR spectra, and consequently Cu^{2+} ions remain the only detectable paramagnetic species. Admission of 15 kPa of CO hardly lowers the intensity of the Cu^{2+} signal. The number of spins detected (5.5×10^{20}

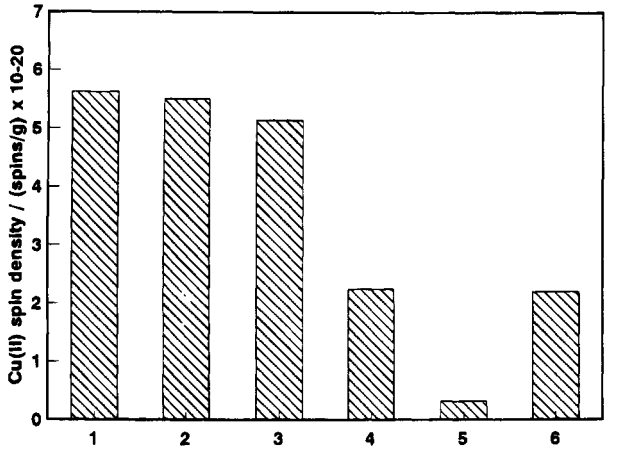

Figure 10. ESR Cu^{2+} spin density of (1) hydrated 12Cu06PdY, (2) after room temperature exposure of (1) to 15 kPa of CO for 10 min and (3) for 60 min; (4) after treatment of (3) at room temperature to *standard* reaction atmosphere for 10; (5) for 60 min; (6) after subsequent heating of (5) to 373 K under the same atmosphere for 60 min.

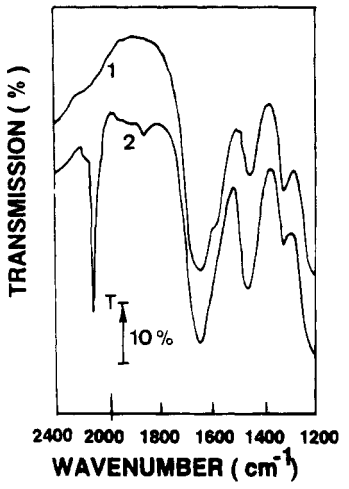

Figure 11. IR spectrum of an active (1) and a deactivated (2) 12Cu06PdY catalyst after CO admission at room temperature.

g^{-1}) is close to the Cu content of the sample (5.9×10^{20} g^{-1}). After 1 h of exposure, only 9% of Cu^{2+} is reduced, while no signals of other paramagnetic species are detectable. During room temperature contact with the reaction atmosphere, the intensity of the Cu^{2+} signal is strongly reduced. IR data (spectra not given) show for such treatment a gradual increase in intensity of the 2121 cm^{-1} band and of the ammonium ion deformation band, at the expense of the intensity of the Pd-ammine N−H deformation. Only when the sample is heated to reaction temperature is the number of Cu^{2+} spins restored for 40%.

The relevance of the intensity of the CO adsorption band at 2121 cm^{-1} for the catalyst activity is further demonstrated by CO adsorption on an active and deactivated catalyst. Figure 11 shows that on a deactivated catalyst the 2121 cm^{-1} band has vanished.

All conclusions obtained for the *standard catalyst* by IR and ESR methods (Figures 7, 8, 10, and 11) are in principle valid for all CuPdY samples, provided their Cu to Pd atomic ratio is 2 or higher. For lower ratios, the behavior of Pd is totally different. Figure 12 compares the IR spectrum of adsorbed CO on the standard sample to a sample containing more Pd. The IR spectrum of the latter sample shows a complex pattern in the ν_{C-O} region which is almost identical to that of reduced PdNaY.[31] A triplet of bands appears now at 2124, 2121, and 2114 cm^{-1}. At the same time the bands around 1970, 1900, and 1830 cm^{-1} have increased in intensity. Sheu et al.[31] have

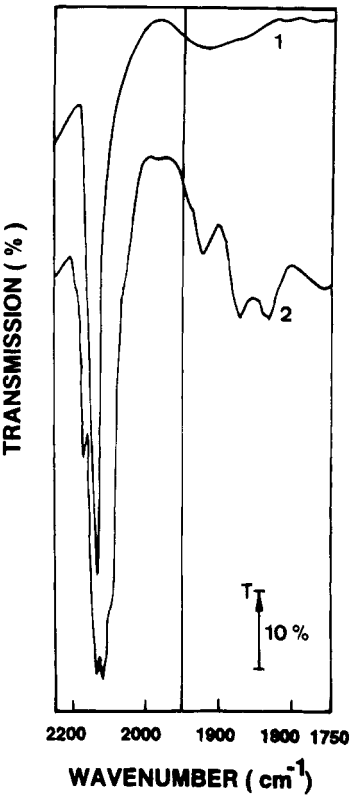

Figure 12. IR spectrum of CO adsorbed on 12Cu06PdY (1) and 09Cu11PdY (2) preexposed to reaction atmosphere (conditions of Figure 2).

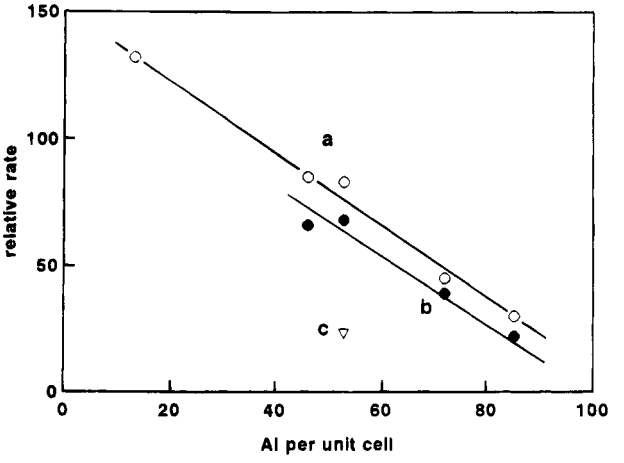

Figure 13. Relative rate over CuPd faujasites with different framework Al density in the Wacker oxidation of ethene (a), propene (b), and 1-butene (c) in the standard conditions of Figure 2.

shown that such spectra are indicative of the existence of Pd_{13} clusters, the size of which is determined by the steric constraints of the faujasite sodalite cage. This clearly indicates that a Y zeolite with a Cu/Pd ratio of 2, contains a maximum number of specific catalytic sites, which can be probed in IR using sorbed carbon monoxide.

Effect of the Al framework Density and the Nature of the Alkene Substrate. In Figure 13 the relative turnover frequency is given in the Wacker oxidation of different alkenes (ethene, propene, and 1-butene) catalyzed by faujasite zeolites with different framework Al density. For ethene and propene, parallel curves show that site efficiency is determined by the framework composition of the zeolite support and therefore by the average electronegativity[33] of the site environment. The lower the Al site density, the higher is the average framework

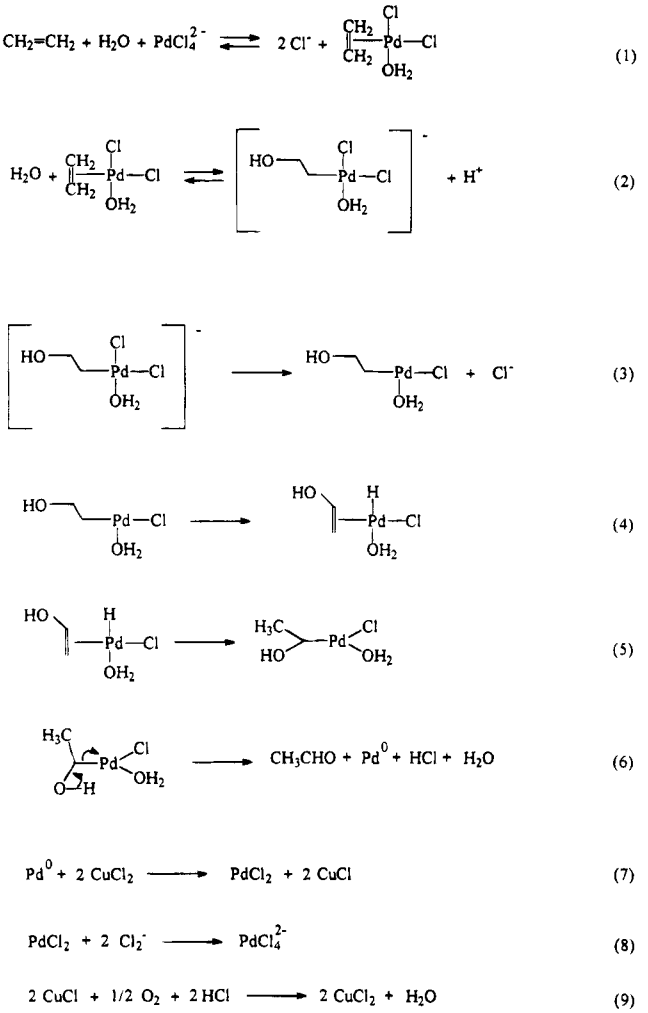

Figure 14. Proven reaction steps for the oxidation of ethene in homogeneous $CuCl_2$–$PdCl_2$ solutions (after ref 23).

electronegativity in terms of, e.g., Sanderson's electronegativity[33,34] and the higher is the Wacker oxidation efficiency per Pd site. This behavior is consistent with the observed reducibility of transition metal ions in zeolites. The higher the average electronegativity of the framework, the higher the transition metal ion reducibility.[35d] This is again in line with the slow reoxidation of Pd^0 by Cu^{2+}.

The relative efficiency of a given site is higher for ethene compared to propene and 1-butene. This sequence is the same with classic Wacker catalysts and reflects the ability of the different Pd coordinated olefines to nucleophilic attack by water.[3b,c]

Discussion

Homogeneous and Heterogeneous Kinetics. The individual steps of the homogeneous Wacker oxidation of ethene have been studied in great detail and are shown in Figure 14. According to Baeckvall et al.,[23] ligand exchanges with water and ethene account for the −2 order in chloride (eq 1), while the nucleophilic attack by external H_2O at Pd coordinated ethene explains the −1 order in acidity (eq 2). The rate-limiting dechlorination (eq 3) is consistent with the first order in ethene and palladium, and the zero order in oxygen. The transformation of coordinated β-hydroxyethyl into α-hydroxyethyl occurs probably via a sequence of β-hydride elimination (eq 4) and migratory insertion (eq 5). Acetaldehyde and Pd^0 are formed from the α-hydroxyethyl σ-complex (eq 6). Finally, Pd^{2+} ions are regenerated with Cu^{2+} (eq 7). Cuprous ions thus obtained are then reoxidized with dioxygen (eq 8). The location of the rate-determining event explains the absence of an isotope effect. The reaction cycle takes into account the lack of isotope incorporation into acetaldehyde from $^{18}O_2$ and ^2H_2O.

There are a number of similarities between the homogeneous catalyst and the CuPdY *standard catalyst*. We have reported[22] the lack of isotope incorporation in acetaldehyde from $^{18}O_2$ and ^2H_2O. We now add the absence of a kinetic isotope effect, the first order in ethene (Figure 4) and the pseudo-first order in Pd (Figure 3), provided the Cu/Pd ratio is at least 2.

In contrast to the homogeneous system, the order in oxygen on the zeolite *standard catalyst* is only zero at high partial pressures and gradually increases to one with decreasing pressure (Figure 4). It should be stressed that most of the prior work with zeolites was done in lean oxygen conditions.

Also at variance with the homogeneous catalyst, the partial pressure of water plays a dominant role as an optimum value is required for maximum catalytic activity. A 4-fold excess with respect to ethene is required for catalyst stability (Figure 5). IR spectroscopy of a deactivating catalyst (Figure 7) proves that in the absence of sufficient water vapor pressure, the Pd complex is deamminated and Cu(II) ions are unable to reoxidize Pd^0. The presence of a larger excess of water results in competitive sorption with the substrate.

Competitive sorption among water and (mixtures of) alkenes is another typical zeolitic feature in Wacker catalysis (Figure 6). The higher Langmuir adsorption coefficient of propene compared to ethene explains the different influence of water in otherwise identical conditions (the order in water for ethene and propene oxidation is −1 and 0.7, respectively) (Figure 5), as well as the strong suppression of the lighter alkene in case alkene mixtures are fed (Figure 6).

Nature of Active Sites. Literature vizualizes the generation of active sites as a formal replacement of the chloro anion of hydrated palladium ions with the anionic zeolite.[9] We derive from the intensity of the δ_{N-H} of Pd-ammine at 1310 cm^{-1} that two residual ammine ligands are present per Pd in a stable catalyst[22] and that such catalyst stands temperatures up to 473 K (Figure 1). Even a $Pd(NH_3)_4^{2+}$-exchanged Y zeolite, degassed below 473 K retains Pd-ammine species.[35] Total removal of the ammine ligands (Figure 2) irreversibly destroys the Wacker activity. The stabilizing effect of ammonia through its coordination with Pd^{2+} may be of thermodynamic origin. This coordination lowers the standard redox potential of the Pd(II)/Pd(0) redox couple, thus inhibiting the agglomeration of Pd^0 into Pd clusters. Alternatively the presence of residual ammonia can prevent the migration of Pd^{2+} from the supercages into the hidden sites of the sodalite cages. Indeed, Homeyer and Sachtler proved that the oxidation of the ammine ligands of $Pd(NH_3)_42+$ in zeolite NaY is a stepwise process producing $Pd(NH_3)_2^{2+}$ ions in the supercages and $Pd(NH_3)^{2+}$ and Pd^{2+} ions in sodalite cages.[36] Only Pd^{2+} can be partially ammoniated, as ammonia addition to a working catalyst leads to a drastic decay in activity. The symmetric N−H deformation of NH_3 coordinated to Cu^{2+} (1275 cm^{-1}) is only found when that of ammonia coordinated Pd (1310 cm^{-1}) has disappeared. This can be rationalized by assuming a decrease of the standard redox potential of the Cu(II)/Cu(I) redox couple, so that it is no longer intermediate between that of Pd(II)/Pd(0) and of O_2/H_2O.

In terms zeolite transition metal chemistry an alternative explanation is possible. The existence of a Cu−Pd−Cu trinuclear complex with hydroxy ions as bridgeheads between Pd and Cu (species **1** in eq 10) would rationalize the existence of a an optimum Cu/Pd ratio in the catalyst (Figure 3) as well

as the existence of a critical water vapor partial pressure for catalyst stability. It further explains the presence of ammonium bands on fresh catalysts, the critical Pd:ammonia stoichiometry of a working catalyst and the specific IR behavior of CO adsorbed on active catalysts (Figure 9 and 11). It is well established that cupric ions in CuY are very susceptible to hydrolysis.[29a] The formation of this trinuclear complex will be highly site-specific. It is therefore not unexpected that only the faujasite topology allows its formation and consequently, generates highly active Wacker catalysts.

$$2Cu^{II} + Pd^{II}(NH_3)_4 + 2H_2O \leftrightarrow \mathbf{1} + 2NH_4^+ \quad (10)$$

$$\mathbf{1} = Cu^{II}-OH-Pd^{II}(NH_3)_2-OH-Cu^{II}$$

The Electron-Transfer Chain: Ethene−Pd−Cu−Dioxygen. Combined IR and ESR spectroscopy of hydrated 12Cu06PdY zeolite after exposure to ethene at room temperature (Figure 7 and 8) shows that Pd^{2+} is reduced to Pd^0 and that transfer of electrons to Cu^{2+} is slow and possibly rate determining. There is ample evidence that in such conditions, Cu^{2+} in CuY is reduced to Cu^+ and not to Cu^0.[37] The reduction of Cu^{II} in CuPdY is not accompanied with the formation of Pd^+, as no such ESR signal is observed. As exposure of this reduced catalyst to oxygen and water leads to a nearly full disappearance of the Cu^{2+} signal and the optimal amount of Cu is about twice that of Pd, eq 11 probably accounts for the equilibration of the different ions.

$$Pd^0 + 2Cu^{2+} \leftrightarrow 2Cu^+ + Pd^{2+} \quad (11)$$

During this process no monovalent palladium species are formed in detectable concentrations (Figure 8), implying that Pd^+ formed under such conditions is unstable and is immediately oxidized to Pd^{2+}. Thus, compared to the fast reduction of Pd^{2+} by ethene in the presence of water, its regeneration by Cu^{2+} and the final electron transfer to O_2 are slow. In conditions of first order in oxygen, the reoxidation of cuprous ions with dioxygen is rate limiting. Only at high partial pressures of oxygen (zero order) the latter step is faster than the reoxidation of Pd^0 with Cu^{2+}. The increasing Wacker oxidation efficiency per Pd site for a lower Al site density of the framework (Figure 13) can be rationalized with this rate-limiting step as the transition ion reducibility in zeolites increases in the same direction.[33d] The reducibility of Cu^{2+} is enhanced as well[33] and, consequently, the oxidation of substrate reduced Pd^{2+} by faujasitic Cu^{2+}.

The same characteristics of the electron transfer chain are revealed upon CO adsorption. All active Wacker catalysts show a unique IR band at 2121 cm^{-1}, with its intensity proportional to the catalytic activity (Figure 9). PdY, CuY as well as CuPdY with Cu/Pd ratio below 2, show distinctly different IR behavior in reaction conditions. This further stresses the existence of a mutual interaction between Pd and Cu in active catalysts and points to the existence of a species like **1**. CO is not an inert diagnostic probe, however. Room temperature CO sorption on a moisture saturated standard CuPdY zeolite forms stoichiometric amounts of CO_2, reduces the intensity of the N−H deformation vibration of Pd-ammine, and generates ammonium ions. Equation 12 rationalizes this, implying that as no ESR evidence for Pd^+ is found, total reduction of Pd occurs. In this equation Z^- stands for the negatively charged zeolite lattice.

$$Pd(NH_3)_4^{2+}(Z^-)_2 + CO + H_2O \rightarrow Pd^0 + CO_2 + 2(Z^-NH_4^+) + 2NH_3 \quad (12)$$

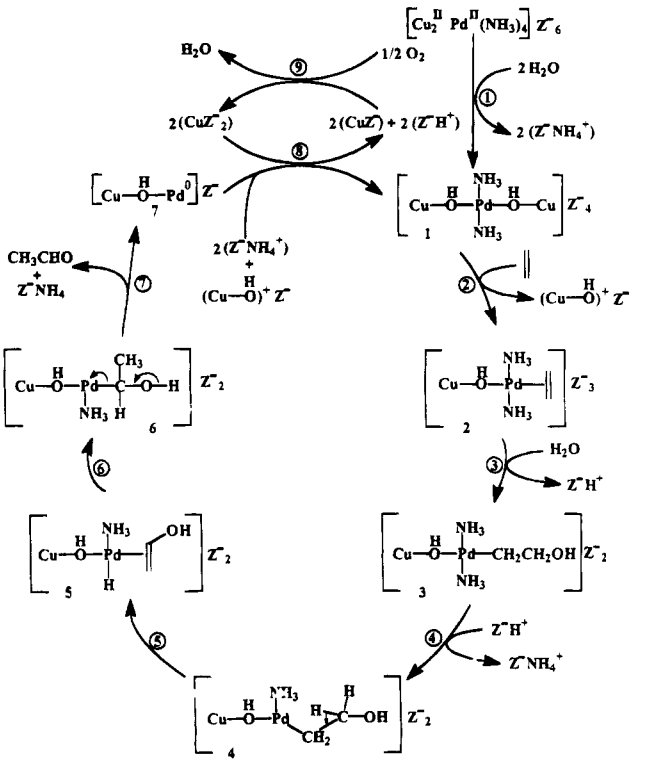

Figure 15. Catalytic cycle for the Wacker oxidation of α-olefins over CuPdY zeolites.

This requires assignment of the 2121 cm^{-1} band to the ν_{C-O} vibration in Pd^0-CO. Although a comparison of literature data seems to impose a high-frequency limit at 2115 cm^{-1} for Pd^0−CO species,[30a,31,38,39] the presence of neighboring copper may easily shift the ν_{C-O} vibration in Pd^0−CO to 2121 cm^{-1}.[40] Moreover, the band intensity increases for longer contact time with CO, when the degree of Pd reduction increases as derived from the intensity of the ammonium band. As in the ESR spectrum of 12Cu06PdY after adsorption of CO no Pd^+ species are observed in detectable quantity, the 2121 cm^{-1} band cannot be assigned to Pd^+-CO species as is done for a band at 2124 cm^{-1} in partially reduced PdY.[31]

After exposure of wet 12Cu06PdY to CO, Pd^{2+} is progressively reduced to Pd^0, while Cu^{2+} remains untouched, as supported by the almost unchanged intensity of the Cu^{2+} ESR signal and the absence of a Cu^+−CO band in the IR spectrum at 2135 cm^{-1}. The appearance of the latter band and the parallel strong reduction of the Cu^{2+} ESR signal can be induced either (i) by heating or (ii) by admission of the reaction atmosphere. Thus the role of Cu as cocatalyst is dual as it enhances the reducibility of Pd^{2+} and allows the regeneration of the Pd^{2+} active site. ESR also shows that room temperature treatment with oxygen of a CO reduced catalyst is unable to reoxidize Cu^+ (Figure 10). In reaction conditions the Cu^{2+} signal is partially restored, indicating once more that the regeneration of Cu^{2+} is slower than the reoxidation of Pd^0.

The Wacker Cycle with Zeolite Catalysts. A cycle for alkene oxidation with dioxygen involving $Cu_{2n}Pd_nY$ zeolites as catalysts is given in Figure 15, based on the arguments advanced in previous paragraphs. The present data clearly show that the rate-limiting step is either the regeneration of Pd^0 by Cu^{II} (step 8) at high oxygen partial pressure or the regeneration of zeolitic cuprous ions by oxygen at low oxygen partial pressures (step 9), rationalizing the observed zero or first orders in oxygen, respectively. Steps 2−7 are equilibrium reactions with respect to the rate limiting events.

The proposed cycle consists in a combination of typical zeolite transition metal chemistry and zeolite-mediated Wacker chemistry. To transform a CuPdY zeolite into an active and stable Wacker catalyst, a Cu/Pd ratio of 2, a critical water vapor partial pressure, and a typical zeolite topology (faujasite) are required (step 1). The proposed trinuclear intermediate **1** takes into account these specificities. Furthermore, it allows the generation of species **7**, which explains the resistence to sintering of Pd^0 atoms. In step 2 ethene coordinates with Pd^{2+} via disruption of the trinuclear species, rather than via a ligand exchange with ammonia, as required by the $Pd:2NH_3$ composition of the working catalyst. The location of step 2 in the cycle with respect to the rate-limiting event explains the first order in ethene and the absence of an isotope effect. The substrate concentration near species **1** is determined by a Langmuir-type relation and in contrast to homogeneous Wacker chemistry, there is no direct proportionality between substrate partial pressure and concentration near the active site. Thus competitive sorption in the zeolite pores is able to modify kinetics (zero order in propene and competition among water and alkene mixtures).

The subsequent steps 3–7 are based on the similarities between homogeneous and zeolite-based Wacker chemistry. Oxypalladation (step 3), β-hydride elimination (step 5), migratory insertion (step 6), and reductive elimination (step 7) occurring on zeolite-modified intermediates all have homogeneous counterparts. The deammination step 4 is comparable to the dechlorination of Pd, which is only rate limiting in the homogeneous case.

Experimental Section

Materials. As starting materials NaY and NaX zeolites with different Si/Al ratios obtained by direct synthesis were used as recieved from Union Carbide Corp. The dealuminated Y sample was from PQ. The framework Si/Al ratio was determined with ^{29}Si MAS NMR.[41] The number of Al ions per unit cell can be extracted from Figure 13. The standard Y zeolite contains 56 framework Al ions per unit cell.

The Na zeolites were first ion-exchanged at 298 K for 24 h using an excess of a 0.01 M aqueous solution of $Cu(NO_3)_2$. The solid/liquid ratio during the ion exchange was 1 g/L. The sample was washed with distilled water until nitrate ions were no longer detected, then dried at 333 K and stored in a desiccator over a saturated NH_4Cl solution. Pd^{2+} ions were exchanged into such Cu-zeolite, with a predetermined amount of aqueous $Pd(NH_3)_4Cl_2$, using the same solid to liquid ratios as for the copper exchange. The samples were now washed with distilled water till chloride free. Chemical analysis showed that all Pd was taken up by the zeolites. In this way a series of Na-Y zeolites with variable Cu/Pd ratios was obtained. ICP analysis of such samples is given in Table 1. The figures preceding the chemical elements in the sample notation refer to the number of cations of these elements present per unit cell.

High-purity helium, oxygen, ethene, propene, and 1-butene from l'Air Liquide were used for catalytic experiments. Ethene-d_4 was from Merck, Sharpe and Dohme. Cu(acetylacetonate)$_2$-Cl_2 was from Ventron.

Methods. The catalytic oxidation of ethene with oxygen was studied in a continuous-flow fixed-bed stainless-steel reactor with an internal diameter of 9 mm, operated at a total pressure of 0.1 MPa and containing 200 mg of catalyst. The standard reaction temperature used was 373 K, unless otherwise specified. The standard space–time used in the reactor (W/F_0, in which W is the amount of catalyst and F_0 is the total molar flow rate at the reactor entrance) was 2.86 kg/mol. The composition of the gas feed was regulated by means of Brooks mass-flow controllers. Water was added to the feed by passing helium and oxygen through a thermostated saturator filled with inert alumina particles. The standard gaseous feed composition used was 41.9 mol % of oxygen, 41.9 mol % of helium, 14 mol % of water, and 2.2 mol % of ethene. On-line analysis at the reactor outlet was performed with a HP 5880 GC, equipped with two columns: (i) a Poraplot Q column (25 m length and 0.53 mm diameter), connected to a FID detector for the determination of the hydrocarbons and oxygenates; (ii) a Porapak R column (3 m length and 32 mm diameter), connected to a methanator and a FID for the determination of CO and CO_2.

TABLE 1: Chemical Composition of the NaY Zeolites Exchanged Subsequently with Cu(II) and Pd(II) Ions

	ions per unit cell			
sample notation	Cu^{2+}	Pd^{2+}	Na^+	Cu/Pd
03Cu02PdY	03.0	01.5	47.0	02.0
06Cu03PdY	06.0	03.0	38.0	02.0
08Cu04PdY	07.5	04.0	33.0	01.9
15Cu02PdY	15.0	01.5	23.0	10.0
14Cu03PdY	14.0	03.0	22.0	04.0
13Cu04PdY	13.0	04.0	22.0	03.3
12Cu06PdY[a]	11.5	06.0	21.0	01.9
10Cu09PdY	10.0	09.0	18.0	01.1
09Cu11PdY	08.5	11.0	16.0	00.8
12Cu06PdF46[b]	12.0	06.0	10.0	02.0
12Cu06PdF70[b]	12.0	06.0	34.0	02.0
12Cu06PdF85[b]	12.0	06.0	49.0	02.0
06Cu03PdF18[b]	06.0	03.0	–	02.0

[a] The standard catalyst. [b] F = faujasite followed by the number of Al per unit cell.

Infrared experiments in the double-beam transmission mode, covering the 2400–1200 cm^{-1} range, were made *in situ* in a Perkin-Elmer 580 B spectrometer using a cell, allowing gas flow over the wafers. Either fresh or used catalysts, as such or after CO adsorption, were examined or the catalytic reaction was simulated.

Temperature-programmed oxidation measurements (TPO), using 50% of oxygen in helium, were performed in a continuous flow reactor, the outlet of which was connected to a computer-steered quadrupole mass spectrometer. The quadrupole was used in the multiple ion monitoring mode.

ESR measurements were carried out on catalyst samples treated for different periods of time with ethene, CO or dioxygen to identify cupric or other paramagnetic species and to monitor their intensity their intensities. ESR spectra were recorded at X-band frequency with a Bruker ESP 300 E spectrometer at 120 K. Cu^{2+} spin density was determined with Cu(acetylacetonate)$_2$.

The zeolite powder was pressed, crushed, and sieved. The particle fraction between 0.25 and 0.50 mm was used in all but the IR experiments. In the latter case, wafers of zeolite powder were pressed with a thickness of 5 ± 0.1 mg/cm^2 of wafer.

Acknowledgment. The authors acknowledge sponsoring of this work in the frame of an IUAP program on Supramolecular Chemistry and Catalysis by the Belgian Ministry of Science Policy. P.E. acknowledges the Flemish National Fund of Scientific Research (NFWO) for a grant as research assistant.

References and Notes

(1) Weisermel, K.; Arpe, H. J. *Industrial organic chemistry*; Verlag Chemie: Weinheim, 1988; pp 174–177.

(2) Aguilo, A. *Adv. Chem. Ser.* **1967**, *5*, 321–346.

(3) (a) Smidt, J.; Hafner, W.; Sedlmeier, J.; Sieber, R.; Ruttinger, R.; Kojer, H. *Angew. Chem.* **1959**, *71*, 176–182. (b) Henry, P. M. *J. Am. Chem. Soc.* **1965**, *87*, 4423–4428. (c) *J. Am. Chem. Soc.* **1966**, *88*, 1595–1597.

(4) Hosokawa, T.; Murahashi, S. I. *Acc. Chem. Res.* **1990**, *23*, 49−54.
(5) Kominiyama, H.; Inoue, H. *J. Chem. Eng. Jpn.* **1975**, *8*, 310−315.
(6) Rao, V.; Datta, R. *J. Catal.* **1988**, *114*, 377−386.
(7) Elleuch, B.; Naccache, C.; Ben Taarit, Y. *Stud. Surf. Sci. Catal.* **1984**, *35*, 139−145.
(8) Kubota, T.; Kumada, F.; Tominaga, H.; Kunugi, T. *Int. Chem. Eng.* **1973**, *13*, 539−545.
(9) Arai, H.; Yamashiro, T.; Kubo, T.; Tominaga H. *Bull. Jap. Pet. Inst.* **1976**, *18*, 39−44.
(10) Eguchi, K.; Tokiai, T.; Arai, H. *J. Catal.* **1988**, *111*, 457−459.
(11) Morikawa, Y.; Ishikawa, S.; Tanaka, H.; Ueda, W. *Proc. Int. Conf. Ion Exchange Processes* **1991**, 139−144.
(12) Van Der Heide, E.; Ammerlaan, J. A. M.; Gerritsen, A. W.; Scholten, J. J. F. *J. Mol. Catal.* **1989**, *55*, 320−329.
(13) Van der Heide, E.; Ammerlaan, J. A. M.; Gerritsen, A. W.; Scholten, J. J. F. *Proc. 9th Int. Congr. Catal.* **1990**, 1648−1655.
(14) Forni, L.; Terzoni, G. *Ind. Eng. Chem. Process Des. Dev.* **1977**, *16*, 288−293.
(15) Evnin, A. B.; Rabo, J. A.; Kasai, P. H. *J. Catal.* **1973**, *30*, 109−117.
(16) Matveev, K. I. *Kinet. Katal.* **1977**, *18*, 862−877.
(17) Vasilevskis, J.; Dedeken, R. J.; Saxton, R. J.; Wentrceck, P. R.; Fellmann, J. D.; Kipnis. U.S. Patents 1988, 4720474, 4738943.
(18) Minachev, Kh. M.; Usachev, N. Ya.; Isakov, Ya. I.; Rodin, A. P.; Kalinin V. P. *Izv. Akad. Nauk SSSR, Ser. Khim.* **1981**, 724−730.
(19) Minachev, Kh. M.; Usachev, N. Ya.; Rodin, A. P.; Isakov, Ya. I. *Izv. Akad. Nauk SSSR, Ser. Khim.* **1982**, 1975−1982.
(20) Minachev, Kh. M.; Usachev, N. Ya.; Rodin, A. P.; Isakov, Ya. I. *Izv. Akad. Nauk SSSR, Ser. Khim.* **1982**, 132−138.
(21) Usachev, N. Ya.; Rodin, A. P.; Khodakov, Yu. S.; Minachev, Kh. M. *Izv. Akad. Nauk SSSR, Ser. Khim.* **1984**, 747−755.
(22) Espeel, P. H.; Tielen, M. C.; Jacobs, P. A. *J. Chem. Soc., Chem. Commun.* **1991**, 669−671.
(23) Baeckvall, J. E.; Akermark, B.; Ljunggren, S. O. *J. Am. Chem. Soc.* **1979**, *101*, 2411−2416.
(24) When competitive sorption of water for ethene occurs in a Langmuir-type rate equation of the form: $r = kbP_{ethene}/(1 + bP_{ethene} + b^*P_{water})$, then a −1 order in water will be observed when $1 + bP_{ethene} < b^*P_{water}$; if the partial pressures of ethene and water are not too different, it follows that that $b^* \gg b$.
(25) In one of the few kinetic studies of hydrocarbon conversion on zeolite Y using "rival model screening" techniques, it was found essential to relate the hydrocarbon pressure in the zeolite pores to the partial pressure in the system via a Langmuir-type expression. See: Steyns, M.; Froment, G. *Ind. Eng. Chem. Prod. Res. Dev.* **1981**, *20*, 660−668.
(26) Flentge, D. R.; Lunsford, J. H.; Jacobs, P. A.; Uytterhoeven, J. B. *J. Phys. Chem.* **1975**, *79*, 354−361.
(27) Water in cation Y zeolites has a dual influence; it enhances the mobility of the cations (Schoonheydt et al.) and retains the bivalent ones in the large cages (Mortier) in the present case in the immediate neighborhood of Pd^{2+}-ammine. (a) Schoonheydt, R. A.; Uytterhoeven, J. B. *Adv. Chem. Ser.* **1971**, *101*, 456. (b) Mortier, W. J. *Compilation of Extra Framework Sites in Zeolites*; Butterworth Scientific: New York, 1982, pp 19−31.
(28) With the integrated intensity for the 1275 cm^{-1} band[27] 90% of the Cu^{II} is found to be coordinated as Cu^{2+}-tetraammine in the deactivated *standard* catalyst.
(29) (a) Jacobs, P. A.; De Wilde, W.; Schoonheydt, R. A.; Uytterhoeven, J. B.; Beyer, H. *J. Chem. Soc., Faraday Trans. 1* **1976**, *72*, 1221−1230. (b) Packet, D.; Schoonheydt, R. A.; *Stud. Surf. Sci. Catal.* **1984**, *18*, 41−51. (c) *J. Chem. Soc., Faraday Trans. 1* **1986**, *28*, 385−393. (d) Schoonheydt, R. A. *Catal. Rev.* **1993**, *35*, 129−168.
(30) In a PdNa-Y first oxidized at 773 K and then room temperature reduced with hydrogen, an ESR signal with $g_{\|} = 2.33$ and $g_{\perp} = 2.10$ was assigned to Pd^{+}; substantial formation of this Pd^{+} species upon ethene treatment would show up in Figure 8, curve 1. Naccache, C.; Primet, M.; Mathieu, M. V. *Adv. Chem. Ser.*, **1973**, *121*, 266−280.
(31) Sheu, L.-L.; Knözinger, H.; Sachtler, W. M. H. *J. Am. Chem. Soc.* **1989**, *111*, 8125−8131.
(32) Huang, Y. *J. Catal.* **1973**, *30*, 187−194.
(33) (a) Mortier, W. J. *J. Catal.* **1978**, *55*, 138−145. (b) Jacobs, P. A.; Mortier, W. J.; Uytterhoeven, J. B. *J. Inorg. Nucl. Chem.* **1978**, *40*, 1919−1923. (c) Jacobs, P. A. *Catal. Rev.* **1982**, *24*, 415−440. (d)Jacobs, P. A. *Stud. Surf. Sci. Catal.* **1986**, *29*, 357−414.
(34) Baekelandt, B. G.; Mortier, W. G.; Lievens, J. L.; Schoonheydt, R. A. *J. Am. Chem. Soc.* **1991**, *113*, 6730−6734.
(35) Zhang, Z.; Sachtler, M. H.; Chen, H. *Zeolites* **1990**, *10*, 784−789.
(36) Homeyer, S. T.; Sachtler, W. M. H. *J. Catal.* **1989**, *118*, 266−274.
(37) (a) Beyer, H.; Jacobs, P. A.; Uytterhoeven, J. B.; Vandamme, L. J. *Proc. Sixth Int. Congr. Catal.* **1976** *1*, p 273. (b) Jacobs, P. A.; Tielen, M.; Linart, J.-P.; Uytterhoeven, J. B.; Beyer, H. *J. Chem. Soc., Faraday Trans. 1* **1976**, *72*, 2793−2804. (c) Jacobs, P. A.; Linart, J.-P.; Nijs, H.; Uytterhoeven, J. B. *J. Chem. Soc., Faraday Trans. 1* **1977**, *73*, 1745−1754.
(38) Rasko, J.; Solymosi, F. *J. Chem Soc., Faraday Trans. 1* **1984**, *80*, 1841−1853.
(39) Palazov, A.; Chang, C. C.; Kokes, R. J. *J. Catal.* **1975**, *36*, 338−350.
(40) When Pd^0 is surrounded by Cu−OH species, which are electronegative, decreased back donation in the antibinding orbitals of CO will occur, resulting in an increase in the ν_{C-O}.
(41) Engelhardt, G.; Lohse, U.; Lippmaa, E.; Tarmak, M.; Märgi, M. *Anorg. Allg. Chem.* **1981**, *482*, 49−64.